



University of
Zurich^{UZH}

Zurich Open Repository and
Archive

University of Zurich
Main Library
Strickhofstrasse 39
CH-8057 Zurich
www.zora.uzh.ch

Year: 2019

A Versatile Biosynthetic Hydrogel Platform for Engineering of Tissue Analogues

Klotz, Barbara J ; Oosterhoff, Loes A ; Utomo, Lizette ; Lim, Khoon S ; Vallmajo-Martin, Queralt ; Clevers, Hans ; Woodfield, Tim B F ; Rosenberg, Antoine J W P ; Malda, Jos ; Ehrbar, Martin ; Spee, Bart ; Gawlitta, Debby

Abstract: For creating functional tissue analogues in tissue engineering, stem cells require very specific 3D microenvironments to thrive and mature. Demanding (stem) cell types that are used nowadays can find such an environment in a heterogeneous protein mixture with the trade name Matrigel. Several variations of synthetic hydrogel platforms composed of poly(ethylene glycol) (PEG), which are spiked with peptides, have been recently developed and shown equivalence to Matrigel for stem cell differentiation. Here a clinically relevant hydrogel platform, based on PEG and gelatin, which even outperforms Matrigel when targeting 3D prevascularized bone and liver organoid tissue engineering models is presented. The hybrid hydrogel with natural and synthetic components stimulates efficient cell differentiation, superior to Matrigel models. Furthermore, the strength of this hydrogel lies in the option to covalently incorporate unmodified proteins. These results demonstrate how a hybrid hydrogel platform with intermediate biological complexity, when compared to existing biological materials and synthetic PEG-peptide approaches, can efficiently support tissue development from human primary cells.

DOI: <https://doi.org/10.1002/adhm.201900979>

Posted at the Zurich Open Repository and Archive, University of Zurich

ZORA URL: <https://doi.org/10.5167/uzh-177709>

Journal Article

Published Version



The following work is licensed under a Creative Commons: Attribution-NonCommercial 4.0 International (CC BY-NC 4.0) License.

Originally published at:

Klotz, Barbara J; Oosterhoff, Loes A; Utomo, Lizette; Lim, Khoon S; Vallmajo-Martin, Queralt; Clevers, Hans; Woodfield, Tim B F; Rosenberg, Antoine J W P; Malda, Jos; Ehrbar, Martin; Spee, Bart; Gawlitta, Debby (2019). A Versatile Biosynthetic Hydrogel Platform for Engineering of Tissue Analogues. *Advanced Healthcare Materials*, 8(19):e1900979.

DOI: <https://doi.org/10.1002/adhm.201900979>

A Versatile Biosynthetic Hydrogel Platform for Engineering of Tissue Analogues

Barbara J. Klotz, Loes A. Oosterhoff, Lizette Utomo, Khoon S. Lim, Queralt Vallmajo-Martin, Hans Clevers, Tim B. F. Woodfield, Antoine J. W. P. Rosenberg, Jos Malda, Martin Ehrbar, Bart Spee, and Debby Gawlitta*

For creating functional tissue analogues in tissue engineering, stem cells require very specific 3D microenvironments to thrive and mature. Demanding (stem) cell types that are used nowadays can find such an environment in a heterogeneous protein mixture with the trade name Matrigel. Several variations of synthetic hydrogel platforms composed of poly(ethylene glycol) (PEG), which are spiked with peptides, have been recently developed and shown equivalence to Matrigel for stem cell differentiation. Here a clinically relevant hydrogel platform, based on PEG and gelatin, which even outperforms Matrigel when targeting 3D prevascularized bone and liver organoid tissue engineering models is presented. The hybrid hydrogel with natural and synthetic components stimulates efficient cell differentiation, superior to Matrigel models. Furthermore, the strength of this hydrogel lies in the option to covalently incorporate unmodified proteins. These results demonstrate how a hybrid hydrogel platform with intermediate biological complexity, when compared to existing biological materials and synthetic PEG-peptide approaches, can efficiently support tissue development from human primary cells.

engineering and regenerative medicine are considered as a potential solution to overcome this problem. Considerable advancements over the course of almost 30 years resulted in therapeutic applications with successes for thin or avascular tissues and organs such as skin,^[1] cartilage,^[2] and bladder.^[3] For biologically complex tissue analogues and for upscaling of constructs to clinically relevant size, a major bottleneck for advancement to the clinical setting lies in the lack of vascularization.^[4] Furthermore, there is a need for clinically relevant, degradable biomaterials that stimulate cell differentiation, matrix secretion and ultimately, functional tissue development.^[5]

Hydrogels play an important role in tissue engineering approaches, since their 3D polymer network, characterized by a high water content, can closely resemble the native extracellular matrix in the

1. Introduction


Shortcomings of autologous tissue transplants and the shortage of donor organs are a major clinical burden to society. Tissue

(developing) tissues. In fundamental stem cell culture, the most commonly used biomaterial is isolated from a mouse tumor (Engelbreth–Holm–Swarm), which is rich in extracellular matrix proteins with the trade name Matrigel (or Cultrex).^[6]

B. J. Klotz, Dr. L. Utomo, Prof. A. J. W. P. Rosenberg, Dr. D. Gawlitta
Department of Oral and Maxillofacial Surgery and Special Dental Care
University Medical Center Utrecht
Utrecht University
3508 GA Utrecht, the Netherlands
E-mail: D.Gawlitta@umcutrecht.nl

B. J. Klotz, L. Utomo, J. Malda, D. Gawlitta
Regenerative Medicine Utrecht
3584 CT Utrecht, the Netherlands

L. A. Oosterhoff, Dr. B. Spee
Department of Clinical Sciences of Companion Animals
Faculty of Veterinary Medicine
Utrecht University
3508 TC Utrecht, the Netherlands

 The ORCID identification number(s) for the author(s) of this article can be found under <https://doi.org/10.1002/adhm.201900979>.

© 2019 The Authors. Published by WILEY-VCH Verlag GmbH & Co. KGaA, Weinheim. This is an open access article under the terms of the Creative Commons Attribution-NonCommercial License, which permits use, distribution and reproduction in any medium, provided the original work is properly cited and is not used for commercial purposes.

DOI: 10.1002/adhm.201900979

Dr. K. S. Lim, Dr. T. B. F. Woodfield
Department of Orthopaedic Surgery and Musculoskeletal Medicine
Centre for Bioengineering and Nanomedicine
University of Otago
Christchurch 8011, New Zealand

Dr. Q. Vallmajo-Martin, Dr. M. Ehrbar
Department of Obstetrics
University Hospital Zurich
University of Zurich
8091 Zurich, Switzerland

Prof. H. Clevers
Hubrecht Institute
Royal Netherlands Academy of Arts and Sciences
University Medical Center Utrecht
3584 CT Utrecht, the Netherlands

Prof. J. Malda
Department of Orthopaedics
University Medical Center Utrecht
Utrecht University
3508 TC Utrecht, the Netherlands

J. Malda
Department of Equine Sciences
Faculty of Veterinary Medicine
Utrecht University
3508 TC Utrecht, the Netherlands

The composition of Matrigel is heterogeneous with more than 1500 different proteins in its makeup, with the most prevalent proteins being laminin, collagen type IV, and entactin.^[7] This material is especially required for biologically demanding cell cultures, such as organoids^[5,8] and vasculogenesis assays.^[9] Its unique biological composition attributes its value for cell culture to the derivation from the basement membrane and allows cells to proliferate and differentiate. The basement membrane forms a specialized extracellular habitat of multiple organ and tissue systems throughout the body, making it an interesting target matrix for recapitulation.

Furthermore, even though Matrigel might appear as an ideal biomaterial from a biological perspective, there are numerous disadvantages that render it unsuitable for clinical application.^[10] High variability in composition and also stiffness, limits the batch reproducibility massively,^[11] with a lot-to-lot similarity of only 53%.^[7] The murine origin of Matrigel will furthermore complicate clinical translation due to immunogenic effects.^[12]

To advance the translation of human tissue analogues to the clinics, new matrices with biological equivalence to the basement membranes are of high relevance. Recent approaches to create these were based on completely defined synthetic hydrogel platforms, coupled with biological components in the form of peptides improving cell adhesion such as RGDs (arginylglycylaspartic acid).^[13] In this study, laminins were chosen for incorporation because these represent the major protein present in Matrigel. Synthetic polymers are advantageous since they are biologically inert and they have highly defined material and mechanical properties. To impart biological characteristics, inert synthetic polymers such as poly(ethylene glycol) (PEG), poly(vinyl alcohol) (PVA), poly-N-isopropylacrylamide (PNIPAAm) require addition of bioactive peptide sequences. For example, in a vascular toxicity screen, a 2D platform based on poly(ethylene glycol) (PEG) and peptides mimicking the functional groups of large ECM molecules (RGDs) outperformed Matrigel in terms of reproducibility and sensitivity.^[13b] The screening assay typically involves cell culture periods for up to 24 h. Also, for stem cell expansion, the tailored PEG-based system with peptides maintained human embryonic stem cell pluripotency during the initial 4 d.^[13b] Further, another group presented an elegant approach to expand and differentiate intestinal stem cells and organoids in a mechanically dynamic PEG-peptide-based hydrogel to foster fibronectin-based adhesion peptides and compared it to Matrigel.^[13a] During culture over 4 d, intestinal stem cells survived and proliferated in the PEG-peptide hydrogels. Another variant of PEG hydrogels, spiked with RGDs and protease-degradable peptides even allowed for 14 d cell differentiation protocols, which resulted in comparable levels of differentiation as cultures in Matrigel.^[13c]

These recent hydrogel developments are great achievements toward finding a clinically relevant replacement for Matrigel by showing biological equivalence. The next step lies in the further development of a tissue-specific tailorable material, which allows for enhanced cell differentiation compared to Matrigel in order to more closely mimic the function of a native tissue. However, due to the low number of biologically active sites in synthetic matrices with spiked peptides,

they have a reduced cell-driven remodeling capacity when compared to natural materials. Stimulating remodeling of the engineered matrix into a mature biologically functional tissue analogue implies successful long-term performance of encapsulated cells.^[8] The native extracellular matrix (ECM) is a dynamic material, which provides residing cells with specific physical and chemical cues via binding sites.^[14] The ECM is ascribed a crucial role in regulating the development, function, and homeostasis of residing cells.^[15] Hence, an ideal scaffold material for engineering of tissues outside the human body will be one that mimics the natural architecture of the targeted tissue, which remains a significant challenge with the current technology.^[14,16]

To bridge the gap between minimalistic approaches of synthetic, defined matrices, and biological materials, novel hydrogels that provide a matrix with intermediate biological complexity are needed for tissue engineering purposes. Gelatin can serve this purpose, as it is derived from the most abundant protein in the human body, collagen type I, which is highly conserved among species. It is associated with less immunogenicity than collagen while retaining bioactive signals of its native progenitor. Furthermore, gelatin is used, despite its animal origin, routinely in the clinics since several decades.^[17]

In this study, we developed a gelPEG hydrogel platform aimed at recapitulating the biological functionality of the basement membranes, while maintaining the simplicity, tailorability, and reproducibility of synthetic hydrogels. This hybrid semisynthetic gelPEG platform uniquely combines its inherent support of cell performance, tailorability of physicochemical characteristics and highly versatile application by incorporation of natural (unmodified) tissue-specific proteins. A systematic material characterization is presented and tailored toward physicochemical parameters favoring multitissue differentiation. The biological performance of the novel hydrogel is compared to that of Matrigel. Vasculogenesis, a hallmark process for tissue engineering, is evaluated in gelPEG hydrogels and assessed regarding extent and maturity of the developed vascular network in 3D. To demonstrate the enhanced cell-instructive capacity of the new basement membrane-inspired material, it was applied in engineering of prevascularized bone and liver-like tissue analogues.

2. Results

2.1. Systematic Evaluation of gelPEG Hybrid Hydrogels

Hydrogels were fabricated by forming covalent crosslinks between gelatin and PEG via an enzymatic reaction with coagulation factor XIII (FXIIIa). To do so, the specific amino acid substrate sequence (NQEQVSPL) of the enzyme was conjugated to 8 arm PEG (PEG-Gln), which can be crosslinked with the native lysine residues on gelatin (**Figure 1**). Moreover, in the same reaction step, other lysine-containing proteins may be coupled into the gelPEG hydrogel network to create a tissue-specific ECM-like environment. Before crosslinking, cells were resuspended in the gelatin-PEG solution to form a 3D polymer network around the cells.

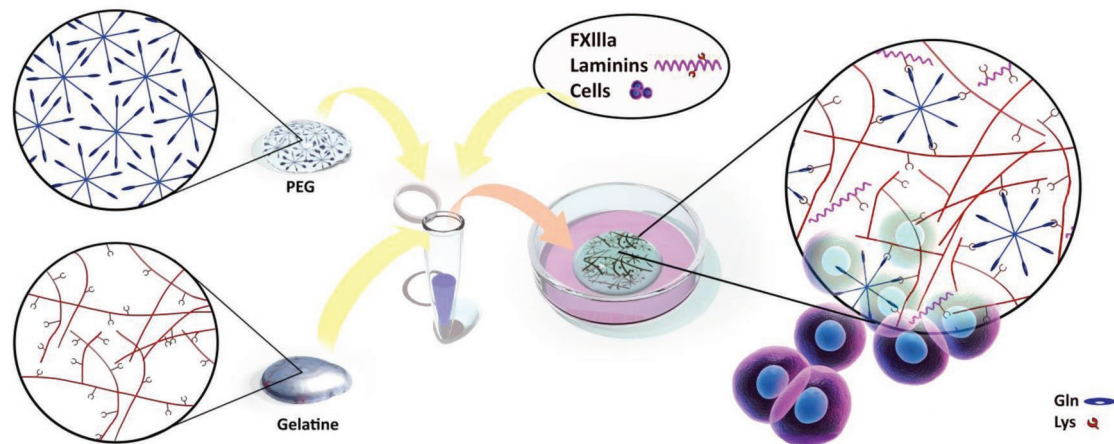


Figure 1. Enzymatic crosslinking reaction between PEG and gelatin. The FXIIIa-specific amino acid sequence for glutamine (gln), NQEQVSPL, was conjugated to 8 arm PEG (PEG-Gln), which can be crosslinked with lysine (lys) residues that are naturally occurring on gelatin. The reaction takes place under physiological conditions and cells can be encapsulated in the same step. It is also possible to immobilize other lysine-containing proteins in the hydrogel network for enhanced tissue specificity (see Figure S2, Supporting Information).

The optimal crosslinking conditions between gelatin and PEG were established by mixing the two components in molar ratios between 1:1 and 6:1 (gelatin)Lys/(PEG)Gln at a constant overall polymer concentration of 3% w/v (**Figure 2**). Hydrogels with the lowest swelling ratio, indicating efficient crosslinking and therefore the best fabrication window, was from 1:1 to 4:1 gelatin/PEG combination (Figure 2a). Since gelatin can be degraded and remodeled by cells, 4:1 gelatin/PEG was preferred over 2:1 and 1:1 and chosen to proceed within further experiments. The swelling ratio decreased with increasing polymer concentration (Figure 2b). A polymer concentration of 1% w/v gelPEG resulted in mechanically unstable hydrogels that could not be manipulated without destruction. The compressive moduli were $2.6 \text{ kPa} \pm 0.6$ for 2% and $6.8 \text{ kPa} \pm 2$ for 3% w/v gelPEG hydrogels with significant differences ($p = 0.0026$) (Figure 2c). Rheological measurements indicated for 2% gelPEG at 4:1 molar ratio a point of gelation after 2 ± 1.5 min and the hydrogel was completely crosslinked after about 15 min (Figure S1, Supporting Information). Furthermore, coupling of lysine-containing proteins of interest into the gelPEG network was demonstrated. To do so, laminin (LN) 521 was successfully incorporated in gelPEG hydrogels as indicated by anti- $\alpha 5$ -LN staining in whole mount constructs (Figure S2b, Supporting Information).

2.2. Vasculogenesis in gelPEG Hydrogels Compared to Matrigel

The biological functionality of the novel developed gelPEG hydrogel for 3D vasculogenesis was assessed and compared to Matrigel, the gold standard for vasculogenesis. Low polymer content or crosslink densities resulting in soft hydrogels are needed to allow for cell migration^[18] and enabling capillary network formation.^[19] For this reason, we chose for this application the 2% w/v gelPEG hydrogel formulation, which is relatively stable (compared to 1%) and still relatively soft.

Interconnected endothelial cell networks from healthy human endothelial colony forming cells (ECFCs) were observed in Matrigel after 3 d, whereas similar capillary-like network took longer to be formed in gelPEG hydrogels and was observed after 6 d (Figure S3, Supporting Information). After a 10 d coculture of healthy human ECFCs and MSCs, highly interconnected vascular-like structures were present throughout all hydrogels ($N = 3$ donor combinations, **Figure 3a,e**; Figure S3c,f, Supporting Information). Quantification of total vessel length and average vessel thickness of 150 μm z-projections revealed comparable network formation in gelPEG and in Matrigel (Figure 3j,k). Also, in both matrices, vascular networks were stabilized by pericyte-like cells as indicated by αSMA staining

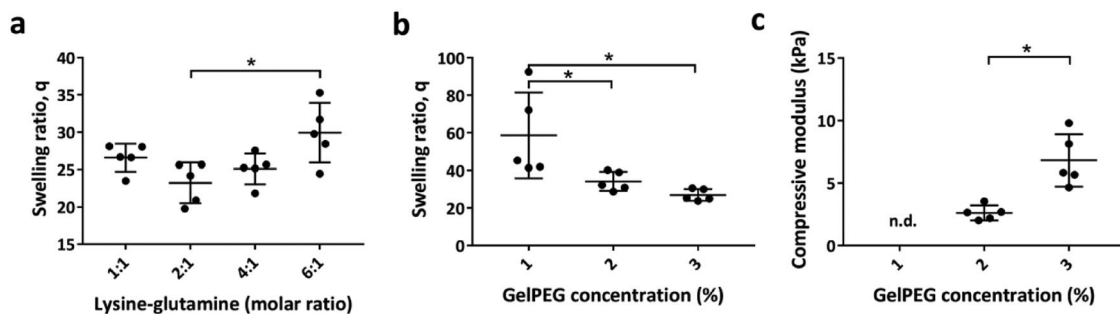


Figure 2. Physical fine-tuning and characterization of gelPEG hydrogels. a) Hydrogels with the lowest swelling ratio were obtained at a molar ratio (gelatin)Lys/(PEG)Gln of 2:1 for 3% w/v gelPEG. b) Decreasing gelPEG concentration resulted in higher swelling ratios. c) Compressive moduli were significantly increased from 2% to 3% gelPEG. n.d., not determined; lys: lysine; gln: glutamine; data are depicted as mean + SD; $n = 5$.

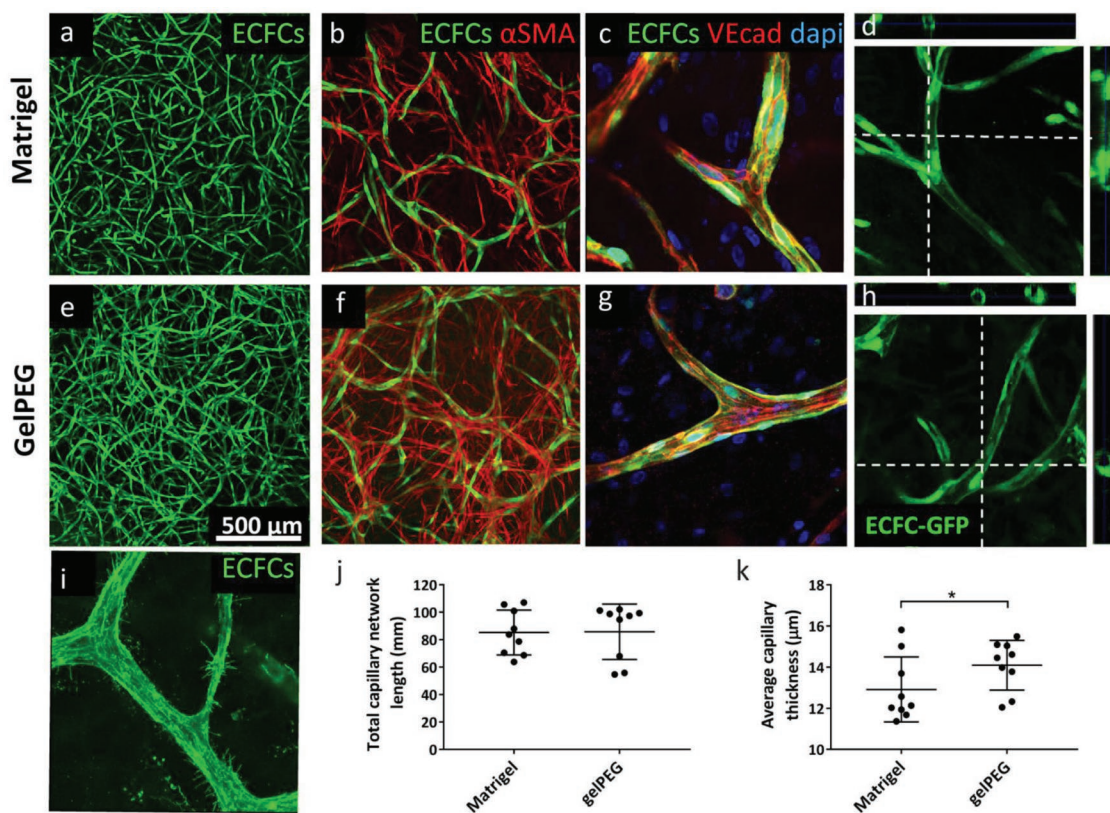


Figure 3. Vasculogenesis in gelPEG and Matrigel characterized by stabilized capillary-like structures with lumen. Human GFP-ECFCs and MSCs were cocultured for 10 d in EGM-2. a,e) Projections of 150 μm confocal stacks through a hydrogel. b,f) Stabilization of vascular networks by pericyte-like cells (red). c,g) Capillary-like structures were composed of multiple fused endothelial cells indicated by cell–cell contact by VE-cadherin junctions. d,h) Capillary-like structures in gelPEG and Matrigel were characterized by lumenization (dotted lines indicate cutting sections). i) Capillary-like structures with filopodia at a site of active angiogenesis, here in a gelPEG hydrogel. j,k) Total vessel length and average vessel thickness in gelPEG hydrogels and Matrigel. Data are depicted as mean + SD; $N = 3$, $n = 3$.

(Figure 3b,f). Moreover, staining of VE-cadherin junctions in the capillary-like structures highlighted the cell–cell contacts of single endothelial cells, which had fused and remodeled into a further matured vessel (Figure 3c,g) containing lumen (Figure 3d,h). A close-up of the capillaries, showed filopodial extensions indicating active angiogenesis at various sites in the hydrogels (here in gelPEG hydrogel) (Figure 3i).

2.3. Development of Prevascularized Bone-Like Tissue Analogues

To further demonstrate the versatility and performance of the novel gelPEG hydrogels, prevascularized bone-like tissue analogues were cultured with human MSCs and ECFCs in the novel material and compared to Matrigel. Prevascularized tissues can be engineered by using endothelial cells that self-assemble into vascular-like networks.^[20] Furthermore, in a vascularized bone engineering approach, MSCs play a dual role. First, a part of these multipotent cells will differentiate into pericyte-like cells, which are needed for stabilization and maturation of capillary networks. Second, another fraction of MSCs will undergo osteogenesis toward the formation of bone tissue.^[19c,21]

To increase gelPEG's biological resemblance to Matrigel, one of its major components, laminin 111 (LN111),^[6b] was immobilized in the gelPEG networks and taken along in the comparison. After a culture period of 2 weeks under osteogenic conditions, ECFC-MSC cocultures were analyzed for markers indicating prevascularization and osteogenesis. From a macroscopic point of view, gelPEG hydrogels became opaque during the culture period, whereas Matrigel remained rather transparent (Figure 4). Matrigel cultures were negative for von Kossa staining, while interestingly, all gelPEG hydrogels were mineralized (Figure 4a,e). Also, gelPEG hydrogels with LN111 showed mineralization in seven out of nine constructs, which appeared more homogeneously distributed throughout the hydrogel when compared to pure gelPEG hydrogels (Figure 4i). The majority of cells in cocultures of all hydrogels were positive for the osteogenic marker osteonectin (Figure 4b,f,j). Late osteogenesis-related genes encoding for osteocalcin and osteopontin were expressed comparably in all hydrogel systems (Figure 4n,o). Moreover, vasculogenesis was present in all hydrogel compositions as shown in projections of 100 μm in the z-direction (Figure 4c,g,k). The total length of the capillary-like network was comparable between Matrigel and gelPEG+LN111, whereas gelPEG hydrogels had a significantly shorter vascular-like network (Figure 4m). The gene expression

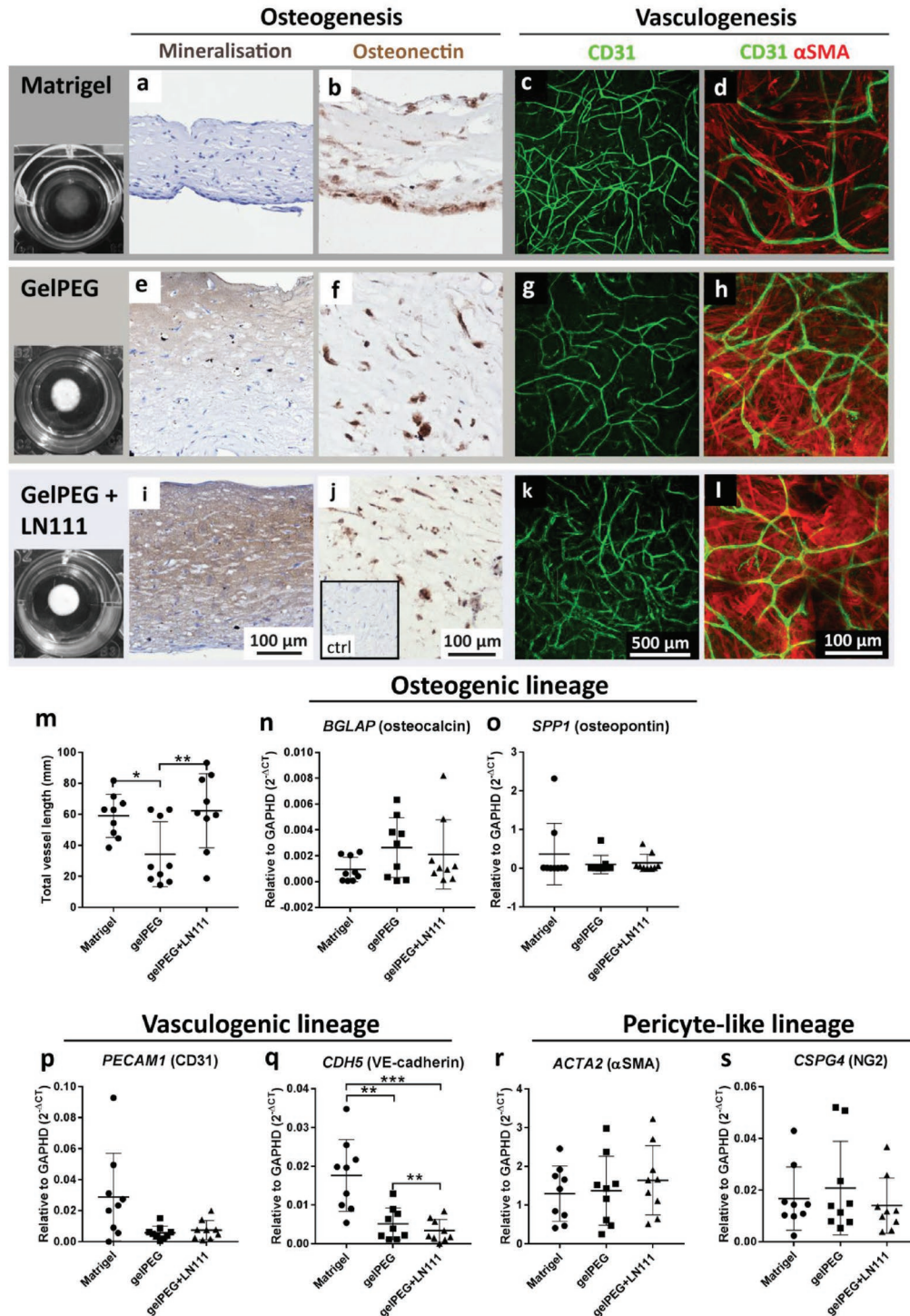


Figure 4. Development of prevascularized bone-like tissue analogues in Matrigel and gelPEG-based hydrogels. ECFC-MSC cocultures were cultured for 2 weeks under osteogenic culture conditions in the different hydrogels before analysis of osteogenesis, vasculogenesis, and presence of pericyte-like cells. Expression of *BGLAP* and *SPP1* as osteogenic markers, *CDH5* and *PECAM1* were measured as endothelial markers and *CSPG4* and *ACTA2* as pericyte markers. a,e,i) Von Kossa staining was positive for gelPEG and gelPEG+LN111 hydrogels highlighting mineralization. b,f,j) Sections of hydrogels highlighted the presence of the osteogenic marker osteonectin in all groups. c,g,k) 100 μ m z-projections of vascular-like networks (green) in the centre of the hydrogels. d,h,l) Vascular-like structures, stabilized by α SMA-positive pericyte-like cells (red). m) Total vessel length was equal in Matrigel and gelPEG+LN111, and significantly longer than in gelPEG hydrogels. n,o) mRNA expression for osteocalcin and osteopontin were comparably expressed in Matrigel, gelPEG, and gelPEG+LN111. p,q) Vasculogenesis-associated genes encoding for CD31 and VE-cadherin were expressed in all hydrogels, with highest VE-cadherin expression in Matrigel, followed by gelPEG and gelPEG+LN111. r,s) Pericyte-associated genes encoding for α SMA and NG2 were equally expressed in all hydrogels. Data are depicted as mean + SD; $N = 3$, $n = 3$.

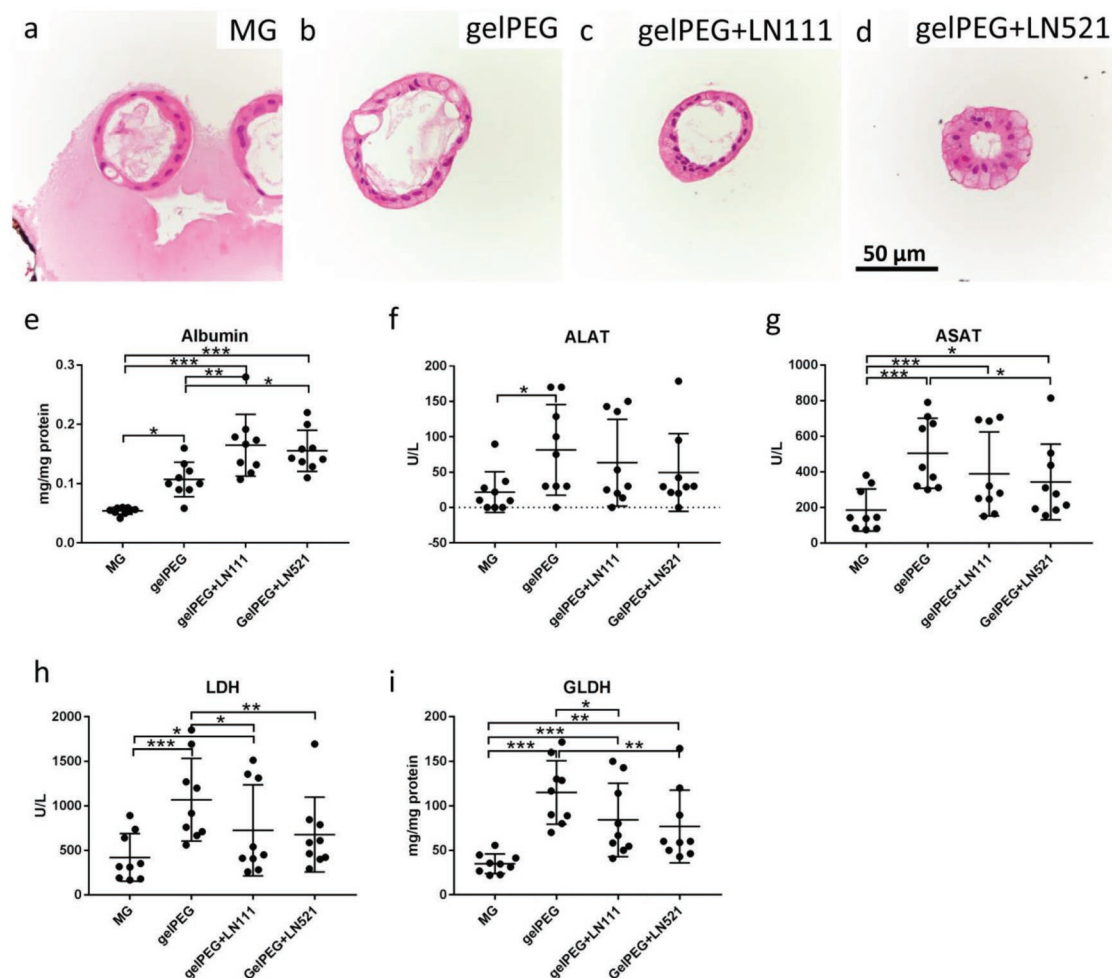


Figure 5. Development of liver-like tissue analogues in Matrigel (MG) and gelPEG-based hydrogels. A functional read-out of protein levels and enzyme activities was performed after 9 d culture of liver organoids. H&E staining of liver organoids in a) Matrigel, b) gelPEG, c) gelPEG+LN111, and d) gelPEG+LN521. e) Albumin protein levels in cultured organoid cell lysates. f,g) ALAT and ASAT enzyme activities of liver organoid cell lysates. h,i) LDH and GLDH enzyme levels of liver organoid cell lysates. Data are depicted as mean + SD; $N = 3$, $n = 3$.

levels encoding for CD31 were comparable between all conditions (Figure 3n). However, the gene expression for VE-cadherin was significantly lower in gelPEG and gelPEG+LN111 compared to Matrigel (Figure 4q). The capillary-like networks were supported by α SMA positive pericyte-like cells (Figure 4d,h,i) and pericyte-related genes encoding for α SMA and NG2 had comparable expression levels in all hydrogel compositions (Figure 4r,s).

Notably, Matrigel constructs lost thickness when compared to gelPEG-based constructs as also apparent in paraffin cross-sections of the constructs (Figure 4a,b,e,f,i,j). At the same time, the diameter of all of the constructs stayed approximately the same (Figure 4, first column).

2.4. Development of Liver-Like Tissue Analogues

To further assess the biological performance of gelPEG hydrogels for biologically demanding cell cultures, liver organoids were encapsulated in tailored hydrogels and compared to a

conventional culture protocol in Matrigel. Since the Matrigel used for this application, typically has a high protein concentration and thus, higher stiffness, in analogy, also gelPEG was used at 3% w/v, to achieve stiffer hydrogels. These hydrogels were further supplemented with LN111, to better resemble Matrigel's composition, or with LN521, since this LN is associated with improved hepatocyte performance.^[22]

Hematoxylin and eosin (H&E) staining of liver organoids in the different matrices highlighted cell structures with similar morphology. However, in gelPEG-based hydrogels, the cell nuclei were located more toward the luminal side of the organoid structures (Figure 5a–d).

Functional readout of the liver-like tissue analogues was performed to investigate the quality of the engineered tissue. In terms of albumin production, liver organoids in gelPEG with added laminins performed best, with levels about 2–3 times higher than in Matrigel (Figure 5e). The liver-like tissues in gelPEG produced significantly higher enzyme levels of alanine aminotransferase (ALAT) and aspartate transaminase (ASAT) compared to Matrigel (Figure 5f,g). Lactate dehydrogenase

(LDH) and the more liver-specific glutamate dehydrogenase (GLDH) indicate metabolic activity of hepatocytes in the different hydrogels. The same trend as observed for the enzyme levels of ALAT and ASAT could be seen for LDH and GLDH. Again, in Matrigel the levels were lowest compared to gelPEG-based hydrogels (Figure 5h,i). Overall, addition of LN111 or LN521 resulted in intermediate enzyme levels, being higher than in Matrigel (Figure 5). Compared to pure gelPEG hydrogels, overall, the addition of LN111 did not further enhance the enzyme levels, whereas LN521 had a slightly negative effect.

The metabolic activity as assessed by Alamar Blue (resazurin to resorufin) conversion by hepatocytes was monitored over culture time showing a steep increase from day 1 to day 3. After a culture period of 9 d, the activity was increased by 50% in Matrigel and gelPEG hydrogels, whereas in LN111 and LN521 containing hydrogels, the activity was doubled when compared to day 1 (Figure S4, Supporting Information).

Furthermore, gene expression levels were quantified on day 9. In contrast to the outcomes on protein level, albumin expression levels were highest in Matrigel and gelPEG and lower in gelPEG when LNs were added (Figure S5b, Supporting Information). *KRT7* (CK7), a cytokeratin that is specifically expressed in simple epithelia and can be used to detect bile ducts in the liver,^[23] was equally expressed in all hydrogels (Figure S5a, Supporting Information). The cytochrome family of enzymes CYP2B6, CYP2C19, and CYP3A4, involved in drug metabolism, e.g., showed comparable expression levels in Matrigel and gelPEG, whereas with the addition of laminins overall lower expression levels were detected (Figure S5d–f, Supporting Information). SLC10A1, which is encoding for a liver-specific sodium/bile acid cotransporter, was comparably expressed in all hydrogels (Figure S5c, Supporting Information).

3. Discussion

In this study, we present a novel, hybrid hydrogel of gelatin and PEG that is easily customized with (native) lysine-containing proteins. The presented tailored hydrogel platform performed as good as Matrigel in terms of 3D vasculogenesis and even outperformed Matrigel when employed for engineering of prevascularized bone- or liver-like tissue analogues.

3.1. Crosslinking of Gelatin and PEG by FXIIIa

The crosslinking strategy that was chosen in this study was compared to a Matrigel control. The main reason for this was that a direct comparison of the biosynthetic gelPEG platform to pure crosslinked gelatins, such as via microbial transglutaminase or UV crosslinked gelatin methacryloyl (gelMA), is inappropriate. The significant differences in the gelatin concentration, hydrogel stiffness, and/or crosslinking density between these systems also affects cell behavior in these materials.

The composition of the herein presented hydrogel-platform is based on a transglutaminase-catalyzed crosslinking mechanism (factor XIIIa), which was adopted from the blood coagulation cascade. The elegant strategy to make use of

the recognition sequences of this enzyme for immobilizing instructive peptides in hydrogels was developed by Hubbell and colleagues at the end of the 1990s.^[24] Subsequently, this mechanism was exploited for crosslinking entirely synthetic PEG hydrogels under physiological conditions.^[25] In this approach, two PEG precursors, one with a glutamine-containing sequence and one with a lysine-containing sequence, served as substrates for factor XIIIa to be coupled.

In this work, we replaced PEG-Lys with gelatin, which natively contains lysine residues that can serve as a donor substrate without any further modifications. We hypothesized that by using a material with inherent cell-responsive elements, a close mimic of the natural environment of cells could be created. In fact, gelatin is a denatured form of collagen, the most abundant protein in the human body.

The crosslinking agent FXIIIa is an FDA approved drug for treating patients with a blood coagulation disorder (trade names are Cluvot, CSL Behring; NovoThirteen, Novo Nordisk). These drug formulations of the enzyme are designed for injection into the blood stream. When applied in the gelPEG system, any potentially remaining activity of FXIIIa could be inactivated by plasmin prior to use for implantation purposes.^[26] Combined, this convincingly highlights the safety of FXIII for hydrogel crosslinking. While PEG is a synthetic polymer, which is on the market for medicinal products,^[27] its conjugated derivatives containing peptides remain to be translated toward the clinics. Furthermore, the incorporated laminins are recombinant and xenogen-free.

3.2. Modular Approach to Integrate Nonmodified Proteins in Hydrogels

Hybrid hydrogels that integrate synthetic and biologic materials, such as ECM-derived materials, are a promising way for synthesizing next-generation hydrogels.^[28] Therefore, the approach of immobilizing ECM-derived proteins in synthetic materials was undertaken by several groups.^[29] Such systems present a merger of both, biological complexity in a physico-chemically controllable matrix. These previous modules of PEG platforms could only accommodate incorporation of ECM molecules of interest after their chemical or biological modification. While being elegant, it can be a laborious approach to modify all proteins of interest.^[30] Therefore, the here taken approach of immobilizing unmodified proteins for tissue specificity presents a simpler hydrogel-platform. Laminins were chosen in this study as model proteins to demonstrate retention of bioactivity after incorporation in gelPEG. Additionally, laminins represent the most abundant protein in Matrigel. The successful incorporation illustrates the flexibility of the platform as tissue-specific isoforms can be used for tailoring the platform's accommodation of various cell types.

3.3. Characteristics of gelPEG Hydrogels

Optimization of the hydrogel composition revealed the best ratio between gelatin and PEG to be between 2:1 and 4:1 to form most effective hydrogels with low swelling ratio and sol

fraction. Increasing the gelatin over PEG concentration still led to reasonable hydrogel formation, an increase of PEG immediately impaired hydrogel formation. This indicates that the availability of lysine residues is the limiting factor in the reaction.

For this study we chose a 4:1 ratio, for which a relatively higher gelatin to PEG concentration ratio was the most ideal. By doing so, less steric hindrance from PEG is expected, which, in contrast to gelatin, cannot be further broken down and replaced by secreted ECM from encapsulated cells. However, the ratio might be further fine-tuned toward a 1:1 Gln:Lys molar ratio, to match the degradation of the hydrogel with the speed of matrix deposition of a specific tissue type of interest. In fact, it was shown previously that degradation of hybrid hydrogels can be further slowed down by the addition of a synthetic polymer.^[31] While for vasculogenic and osteogenic cocultures, gelPEG hydrogels roughly retained their initial volume over culture time, this was not the case for Matrigel-based cocultures. Also, Matrigel constructs of liver organoid cultures appeared very instable after a culture period of 9 d, which was less apparent in gelPEG hydrogels. For further fine-tuning toward upscaled, clinically relevant approaches for liver organoids, it might be therefore suggested to slightly increase either the total polymer or PEG-Gln concentration.

Matrigel has a low and highly variable elastic modulus, ranging from ≈ 0.4 to 3 kPa.^[32] The 2% gelPEG hydrogels with a compressive modulus of $2.6 \text{ kPa} \pm 0.6$ were the closest possible (low protein content) Matrigel mimics from a mechanical point of view that could be created. This comparable stiffness of the materials rules out its potential role as effector of the observed cell behavior.

3.4. Vasculogenesis in gelPEG Matrices

Clinically relevant-sized tissue analogues generally require a prevascular network before implantation. The presence of such an engineered capillary-like network throughout the construct can accelerate the connection with the patients' own vasculature, which is critical for implant survival.^[33] Especially Matrigel is known for its proangiogenic properties that allow for the fast formation of a vascular-like network. Due to this reason it is an often used, highly potent material for vasculogenesis/angiogenesis-related assays.^[11,34]

Prevascular network development over time by human ECFCs was initially favored in Matrigel compared to gelPEG. A thickening of capillary-like structures might indicate further maturation (i.e., arteriogenesis).^[35] In this study, maturity of the networks was shown by the presence of stabilized capillary-like structures and by the presence of lumen. The initial difference in performance between Matrigel and gelPEG might be explained by the proangiogenic properties of Matrigel, which are mediated by proteins such as collagen type IV and LN111^[9,36] that might enable faster vasculogenesis. This assumption is supported by this work where addition of LN111 to osteogenic cultures resulted in improved vascular structure formation. All in all, the gelPEG hydrogel performed equally well as the gold standard Matrigel in terms of long-term prevascularization, both in extent and in maturity.

3.5. Engineering Prevascularized Bone-Like Tissue Analogues

Following, a bone-like construct was engineered as a model tissue, which requires simultaneous development of a prevascular network during bone forming. Early osteogenic differentiation on the protein level of all hydrogel constructs was shown by the presence of osteonectin. Comparable gene expression levels for osteopontin and osteocalcin indicated a comparable extent of osteogenic differentiation in all conditions. However, mineralization, a late phenomenon during osteogenesis, was only present in gelPEG-based hydrogels. While it is known from literature that osteogenesis is supported by Matrigel,^[37] the presence of mineralization becomes generally prevalent after 21 d of culture.^[38] Therefore, the absence of mineralization in MG after 14 d culture is in agreement with literature. Whereas nine out of nine gelPEG hydrogels were characterized by mineralization after only 14 d, seven out of nine gelPEG+LN111 hydrogels were positive for von Kossa staining. Pure gelPEG hydrogels strongly supported early matrix mineralization, which can be explained by the gelatin extraction method. Gelatin is characterized by nucleation sites. Especially, anionic gelatin (obtained by alkaline extraction) enables pronounced calcium binding of the matrix due to its negative charge at physiological pH.^[39] Therefore, due to the nature of the gelatin in gelPEG hydrogels, the matrix is especially favorable as a template for bone development.

The addition of LN111 to gelPEG hydrogels led to an enhanced and more homogenous distribution of minerals throughout the matrix. At the same time, vasculogenesis was stimulated as indicated by a significantly longer vascular network length. LN111 was shown to enhance vasculogenesis, which corresponds to literature.^[9] The influence of LN111 on osteogenesis, especially on mineralization via inducing calcium phosphate precipitation, was established in previous studies.^[40] Together, gelPEG hydrogels appeared as suitable templates for bone development, in which bioactives can enhance tissue development. Specifically, LN111 can be a potent stimulator of vasculogenesis in these constructs. Further fine-tuning of the LN111 concentration, all or not combined with additional factors, might help to optimize the balance between enhanced vasculogenesis and robust mineralization of all hydrogel constructs.

VE-cadherin is an endothelial cell–cell contact marker^[41] and has a key role in endothelial barrier function and angiogenesis.^[42] While the highest VE-cadherin expression is apparent in Matrigel, it might be plausible that downregulation of VE-cadherin in both gelPEG groups was a result of a more complete maturation status of the cells in the prevascular structures, supported by the apparent staining of CD31 and α SMA.

In contrast to purely vasculogenic cultures, vasculo-osteogenic cultures resulted in significantly lower vascular network length in pure gelPEG hydrogels compared to Matrigel. This difference can be explained by the added medium. For the osteogenic differentiation with simultaneous vasculogenesis, osteogenic medium was used instead of vasculogenic medium. Thus, in this condition, ECFCs obtain vasculogenic signals from the embedded MSCs^[43] and not from the medium. Therefore, when the vasculogenic stimulation is not induced by the

culture medium, adequate vascularization can be achieved by incorporation of LN111 in the hydrogel.

The novel gelPEG hydrogel platform allowed for the successful engineering of prevascularized bone-like tissue analogues. Due to the faster osteogenic differentiation while maintaining simultaneous vasculogenesis, gelPEG hydrogels even outperformed Matrigel for engineering of prevascularized bone-like constructs.

3.6. Engineering Liver-Like Tissue Analogues

GelPEG was tested with hepatic organoids^[44] to evaluate the potential in comparison to the gold standard, Matrigel. Overall, the addition of LN111 or LN521 did not show a beneficial effect over pure gelPEG hydrogels, apart from albumin expression. However, compared to Matrigel, gelPEG with added laminins improved liver organoid differentiation as shown by elevated albumin expression and both ALAT and ASAT activity levels. This positive effect of LN521^[22] and in a mix with LN111, was described previously where efficient hepatocyte differentiation and self-organization occurred on laminin-coated surfaces on pluripotent stem cells.^[22a] Especially with respect to metabolic function and self-organization of hepatocytes, LN coatings outperformed a Matrigel control. The minor negative effect of the addition of LN521 on hepatic enzymes and CYP-expression compared to gelPEG alone is in contrast with reports by others.^[22] Since the addition of the LN521 in the pluripotent stem cells is already at the endodermal differentiation stage, this indicates that the effect is not as profound on hepatic organoids which are considered a more mature stem cell type.^[45]

Furthermore, hepatocyte metabolic activity was strongly affected in the different hydrogel compositions. From day 1 until day 3 the cell activity doubled in Matrigel and gelPEG hydrogels, and increased 3.5 and 6 times in hydrogels laden with LN111 and LN521, respectively. This increase in metabolic activity might correlate with cell proliferation. It has been shown that laminins are supporting survival and proliferation of multiple cell types. This strong increase in metabolic activity in gelPEG hydrogels compared to Matrigel in the beginning of the culture period might be due to enhanced proliferation, stimulated by the comparably stiff gelPEG hydrogels. It was shown by Gjorevski et al., that a higher matrix stiffness in PEG hydrogels was associated with intestinal stem cell proliferation, whereas softer hydrogels were needed for cell differentiation.^[13a] The authors also demonstrated that matrix-metalloproteinase (MMP)-sensitive PEG hydrogels (with RDG-sites) could not be degraded fast enough by the cells to allow for organoid differentiation after an initial proliferation phase. Consequently, they added a hydrolytically degradable polymer to the PEG platform to speed up the degradation process after an initial proliferation phase. In the present hydrogel system, combining gelatin and PEG, this cell-mediated degradation and remodeling of the matrix might occur naturally. After reaching a higher cell number during the initial proliferation phase, secreted MMPs might speed up the degradation process, resulting in a softer hydrogel, suitable for cell differentiation. This assumption can be supported by the fact that after the initial 3 d the metabolic

activity gradually dropped in all hydrogel compositions, which might indicate a phase of cell differentiation.

Furthermore, it was shown recently that natural matrices were characterized by fast stress relaxation properties, a feature that synthetic hydrogels are typically missing and which appeared to be critical in guiding cell differentiation.^[46] By using hybrid hydrogels as presented here, this natural characteristic of the extracellular matrix might be present and could have contributed to the permission of multiple cell differentiation into the vasculogenic, osteogenic, and hepatocyte lineages.

The use of gelPEG hydrogels was demonstrated here for the biological suitability as extracellular matrix of multiple tissue engineering approaches. In the future, gelPEG might also be used as a “bioink” for biofabrication processes due to its fast crosslinking.^[47] In combination with reinforcing materials, such as offered by thermoplastics,^[48] complex and multitissue type tissue analogues might be realized. Furthermore, these complex biofabricated tissue constructs might be characterized by a multiscale vascular tree consisting of engineered macrovessels and self-assembled capillary-like structures^[21b] throughout the construct.

4. Conclusions

This research demonstrates that a simple hydrogel composed of gelatin and PEG can replace and even outperform Matrigel for complex, long-term tissue engineering approaches. With this, a clinically relevant, degradable biomaterial was developed, which can efficiently support cell differentiation and matrix secretion toward the development of functional tissue analogues. Moreover, this novel gelPEG platform is easily tailorable with (combinations of) lysine-containing proteins to establish a tissue-specific matrix; illustrated here by addition of tissue-specific laminins. Additional ECM-mimicking cues can prove valuable to create spatial resolution in a hydrogel when aiming at multiple tissue types within one biomaterial, sharing one culture medium.

The presented hybrid hydrogel can be readily applied to other tissue engineering approaches by fine-tuning the ratio between gelatin and PEG, the total polymer concentration, and by covalently immobilizing relevant proteins to further stimulate tissue development. Taken together, we suggest that such hybrid hydrogels consisting of PEG-Gln and a relevant biologic material, catalyzed by FXIIIa, will help to overcome the biomaterial-associated bottleneck of implementing complex tissue engineering in the clinics.

5. Experimental Section

Materials: Alkaline treated porcine skin gelatin (beMatrix™ LS-H high bloom, Nitta Gelatin NA Inc) with an endotoxin count less than 10 endotoxin units (EU) g⁻¹ was used. The gelatin was set to a pH of 7.5, sterile filtered and freeze dried. The peptide was purchased from NeoMPS (Strasbourg, France). Eight-arm PEG-vinyl sulfone (8-PEG-VS, mol wt 40 kDa) was obtained from NOF Europe (Grobendonk, Belgium).

Synthesis of PEG-Gln Macromeres: PEG-Gln was synthesized and characterized as described previously.^[25,49] In brief, a glutamine acceptor substrate (H-NQEQVSPL-ERCG-NH₂, TG-Gln) was used. The

NQEQVSPL cassette corresponds to a substrate site of FXIII in an α 2-plasmin inhibitor^[24b] and the ERCC cassette contains a cysteine that can react with VS.^[50] This TG-Gln substrate was coupled to 8-PEG-VS via Michael-type addition at a 1.2-fold molar excess of TG-Gln to PEG-VS in 0.3 M triethanolamine (pH 8.0) at 37 °C for 2 h. The reaction product was dialyzed, freeze dried, and PEG-Gln conjugation was confirmed by ¹H NMR.

Formation of Gelatin-PEG Hydrogels: Factor XIII (200 U mL⁻¹, Cluvot, CSL Behring) was activated with 20 U mL⁻¹ thrombin (Baxter) in the presence of 2.5 × 10⁻³ M CaCl₂ for 15 min at 37 °C and stored at -80 °C in small aliquots (FXIIIa). Hydrogel formulations consisting of different ratios of PEG-Gln and gelatin were formulated in tris-buffered saline (TBS, pH 7.6, 40 × 10⁻³ M) containing 50 × 10⁻³ M calcium chloride. Hydrogel crosslinking was initiated upon addition of 10 U mL⁻¹ factor XIIIa. For biomaterial characterizations, disc-shaped hydrogels with 8 mm diameter were prepared in a silicone sheet with 1 mm height (BioPlexus Corporation). The reaction mixture was left to crosslink for 1 h in a humidified incubator when covalent crosslinks were formed between native lysines of gelatin or extracellular matrix-derived proteins and the Gln-conjugates on PEG (Figure 1).

Hydrogel Mass Loss and Swelling Analysis: GelPEG hydrogels were prepared in various lysine (Lys) and Gln molar ratios (Lys:Gln) ranging from 1:1 to 6:1 for a 3% w/v total polymer concentration and swelling analysis was performed. Furthermore, gelPEG hydrogels were prepared at a polymer concentration of 1 and 2% w/v at a ratio of 4:1. All hydrogels were characterized by means of swelling and mass loss studies, as described previously^[51] for *n* = 5 technical replicates. In brief, immediately after crosslinking, the wet weight of the hydrogels was measured (*m*_{initial, t=0}). Per experimental group, 10 gels were prepared, from which five were directly frozen, lyophilized, and weighed (*m*_{dry, t=0}) and the other five were incubated in TBS for 24 h at 37 °C before the wet weight (*m*_{swollen}) and the dry weight were determined (*m*_{dry, t=1}). The sol fraction describes the polymer concentration that is not crosslinked into the network and is therefore lost during hydrogel swelling. The hydrogel swelling ratio (*q*) and the sol fraction were calculated according to the following Equations (1–4)^[52]

$$\text{Actual macromer fraction} = \frac{m_{\text{dry}, t=0}}{m_{\text{initial}, t=0}} \quad (1)$$

$$m_{\text{initial, dry}} = m_{\text{initial}, t=0} \times \text{actual macromer fraction} \quad (2)$$

$$\text{Sol fraction} = \frac{m_{\text{initial, dry}} - m_{\text{dry}, t=1}}{m_{\text{initial, dry}}} \times 100\% \quad (3)$$

$$q = \frac{m_{\text{swollen}}}{m_{\text{dry}, t=1}} \quad (4)$$

Rheological Analysis of Hydrogel Formation: The crosslinking of gelPEG hydrogels at 2% w/v and 4:1 ratio by 10 U mL⁻¹ FXIIIa was investigated (*n* = 3). An AR G-2 rheometer (TA-Instruments, the Netherlands) was used with the software TA Instruments Trios V4.3.0.38388. The testing was performed at 0.1% strain and 1 Hz continuous oscillation at 37 °C for 30 min under a humidified atmosphere. The point of gelation of the reactions was measured by recording the time when the shear storage modulus (*G'*) was equal to the shear loss modulus (*G''*) by analyzing $\tan \delta = G''/G'$. *n* = 3 independent measurements were performed.

Mechanical Properties of Swollen Hydrogels: The elastic modulus of the hydrogels was determined after equilibration for 24 h in PBS at 37 °C. By means of a dynamic mechanical analyzer (DMA 2980, TA instruments) compression was applied between -20% per min and -30% at room temperature (RT). The elastic modulus was based on the slope from the linear region of the stress-strain curve of a strain range between 5% and 10% (*n* = 5 technical replicates).

Coupling of Laminins into gelPEG Hydrogels: To investigate the coupling of lysine containing proteins into the gelPEG hydrogel network, laminin 521 (Biolamina, Sweden) served as a model protein. Laminin 521 (LN) was added at a concentration of 10 μg mL⁻¹ to the reaction mixture of 3% w/v 4:1 gelPEG in TBS (*n* = 5 technical replicates). Hydrogels without LN served as a control (*n* = 5 technical replicates). Hydrogel discs (≈1 × 5 mm) of 20 μL volume were incubated for 24 h at 37 °C in TBS. All hydrogels were washed and fixed in 4% formalin and stained with a primary anti-LN α 5 antibody (1:260, clone 4C7, MAB1924, Merck), followed by a goat-antimouse antibody Alexa Fluor 546 (4 μg mL⁻¹, A-11 003, Thermofisher). Imaging of control and LN-laden hydrogels occurred with a fluorescence microscope (BX51, Olympus).

Cell Isolation, Culture, and Characterization: Multipotent mesenchymal stromal cells (MSCs) were derived from human bone marrow aspirates from the iliac crest of three patients after ethical approval and informed consent (University Medical Center Utrecht, 08-001-K). The white mononuclear cell (MNC) fraction was separated via density gradient centrifugation on Ficoll-paque PLUS (1.077 g mL⁻¹, GE healthcare). The collected cells were expanded in expansion medium composed of α -MEM (Gibco), 10% v/v heat-inactivated fetal bovine serum (FBS, Lonza), 100 U mL⁻¹ penicillin, 10 mg mL⁻¹ streptomycin (Gibco), 0.2 × 10⁻³ M L-ascorbic acid-2-phosphate (ASAP, Sigma) and 1 ng mL⁻¹ basic fibroblast growth factor (bFGF, 233-FB R&D Systems), at 37 °C / 5.0% CO₂. MSCs were identified by their capacity to undergo differentiation toward the osteo-, adipo-, and chondrogenic lineages. Furthermore, fluorescence-activated cell sorting (FACS) characterization of the MSCs was performed showing absence of the hematopoietic markers CD14 (RPA-M1, fluorescein isothiocyanate (FITC)-conjugated, Abcam), CD34 (4H11, AP-conjugated, Abcam), CD45 (MEM-28, PE-conjugated, Abcam), and CD79a (HM47, PE-conjugated, Abcam) and presence of the established MSC-like markers CD90 (5E10, FITC-conjugated, Abcam), CD105 (MEM-226, AP-conjugated, Abcam), and CD73 (AD2, PE-conjugated, Abcam). Cells were used up to passage 4.

Human endothelial colony forming cells (ECFCs) were derived from three human umbilical cord blood donors after caesarean sections according to the local ethical guidelines (University Medical Center Utrecht, METC 01-230/K). The obtained cord blood was diluted 1:1 with PBS 2 × 10⁻³ M EDTA before density gradient centrifugation on Ficoll-paque. The harvested cells were cultured on rat collagen type I (Corning) at a seeding density of 10–20 × 10⁶ cells cm⁻². Endothelial growth medium-2 (EGM-2) was composed of endothelial basal medium-2 (EBM, Lonza), 10% v/v FBS, 100 U mL⁻¹ penicillin, 10 mg mL⁻¹ streptomycin and EGM-2 singlequots (Lonza). During the first 7 d after isolation, the medium was refreshed daily. Colonies with cobblestone-like morphology were picked after 14–21 d and were further expanded. ECFCs were characterized by FACS where they were positive for CD105 and CD31 (TLD-3A12, FITC-conjugated, Abcam), partially positive for CD34 and CD309 (VEGFR/KDR, PE-conjugated, MACS Miltenyi Biotech) and negative for CD45, CD14, and CD133 (AC133-VioBright, FITC-conjugated, Miltenyi Biotech). ECFCs were used up to passage 10. Furthermore, ECFCs were transduced with green fluorescent protein (GFP) in a pHAGE-2 vector with a human EF-1 α promoter as described previously.^[21b]

Human liver organoid cultures were generated from three donors from surplus material of donor livers used for liver transplantations performed at the Erasmus Medical Centre Rotterdam (courtesy of Dr. Luc van der Laan, approved by the Medical Ethical Council of the Erasmus MC).^[45]

The organoids were grown in Matrigel in Expansion Medium (EM), as previously described by Huch et al.^[45] A total of 7 to 5 d prior to differentiation toward hepatocyte-like cells the EM was supplemented with 25 ng mL⁻¹ BMP-7 (Peprotech, London, UK). At day 0, the organoids were passaged with a split rate of 1:1 and reseeded in 3% w/v 4:1 gelPEG or Matrigel (Corning, 354 230, Growth Factor Reduced Basement Membrane Matrix). Differentiation medium (DM) containing advanced DMEM/F12 (Gibco, Dublin, Ireland) supplemented with 1% v/v Penicillin-Streptomycin (Thermo Fisher Scientific, Waltham, MA, USA), 1% v/v N2, 1% v/v B27, 10 × 10⁻³ M HEPES, 1% v/v Glutamax,

50 ng mL⁻¹ EGF (all from Invitrogen, Carlsbad, CA, USA), 1.25 × 10⁻³ M N-acetyl cysteine (Sigma-Aldrich, St Louis, MO, USA), 5 × 10⁻⁶ M A83-01 (Tocris Bioscience, Bristol, UK), 25 ng mL⁻¹ HGF, 10 × 10⁻⁹ M Gastrin, 25 ng mL⁻¹ BMP7 (all from Peprotech), 10 × 10⁻⁶ M DAPT (γ-secretase inhibitor, Selleckchem, Houston, TX, USA), 100 ng mL⁻¹ FGF19 (R&D Systems, Minneapolis, MN, USA), and 30 × 10⁻⁶ M dexamethasone (Sigma-Aldrich) was added freshly every other day until the samples were collected (day 9).

MSC-ECFC Coculture in Hydrogels: MSCs and ECFCs were coencapsulated in gelPEG (2% w/v 1:4) hydrogels or Matrigel (Corning, 354 230, Growth Factor Reduced Basement Membrane Matrix) reaching a final seeding density of 5 × 10⁶ MSCs and 1.25 × 10⁶ ECFCs per mL gel. Besides CaCl₂, TBS, and FXIIIa, the reaction mixture contained 20% of cell culture medium. Furthermore, cocultures were encapsulated in Matrigel which was 1:1 diluted with TBS including 20% of cell culture medium.

For vasculogenic cultures, GFP-labeled ECFCs were used. For each condition, three hydrogel droplets of 75 μL each were placed in the center of wells in a 12-well plate. To track formation of capillary-like structures over culture time, hydrogels were imaged on days 2 and 6 using an inverted fluorescence microscope (IX53 Inverted Fluorescence Microscope, Olympus). Hydrogels were cultured in EGM-2 for 10 d, fixed in formalin, and cut in three pieces for different stainings. MSCs from three different donors were combined with GFP-ECFCs from one donor ($N = 3$ different donors, $n = 3$ technical replicates).

To induce osteogenesis and simultaneous vasculogenesis, hydrogels were prepared as for vasculogenic cultures. MSC-ECFC cocultures in gelPEG and gelPEG combined with 10 μg mL⁻¹ laminin 111 were compared to cultures in Matrigel. The cocultures were cultured in osteogenic differentiation medium (ODM) for 2 weeks. ODM was composed of α-MEM, 10% FBS, 100 U mL⁻¹ penicillin, 10 mg mL⁻¹ streptomycin, 10 × 10⁻³ M β-Glycerolphosphate (Sigma), and 10 × 10⁻⁹ M dexamethasone (Sigma). Six hydrogels per condition were prepared, of which three were used for qPCR analysis and three were fixed, cut and used for paraffin embedding and whole mount fluorescent stainings. All experiments were performed with three MSC-ECFC combinations from different donors ($N = 3$, $n = 3$).

Liver Organoid Culture in Hydrogels: Liver organoids from three different donors were encapsulated in Growth factor reduced Matrigel (456 231, Corning, New York, NY, USA), 3% w/v 1:4 gelPEG, gelPEG with 10 μg mL⁻¹ LN111, or gelPEG with 10 μg mL⁻¹ LN521. The gelPEG-cell mixture contained 20% medium, whereas Matrigel was used undiluted. Hydrogel droplets with a volume of 40 μL were placed in the center of culture wells and DM media was added. On days 1, 3, 6, and 9 of differentiation the viability of the organoids was measured with an Alamar Blue assay according to the manufacturer's guide (Invitrogen). A total of 9 days after differentiation samples were collected for gene-expression profiling and enzyme measurements. For gene-expression profiling, organoids were lysed with 350 μL RLT (Qiagen, Hilden, Germany) and stored at -20 °C until further analysis. For enzyme measurements, organoids were lysed in Milli-Q water (Merck Millipore) at -20 °C until analysis. ALAT, ASAT, LDH, GLDH, albumin, and total protein were measured using the AU680 Beckman (Beckman Coulter, Brea, CA, USA) standard protocols, and values were corrected for total protein levels ($N = 3$, $n = 3$).

mRNA Isolation, cDNA Synthesis, and qPCR Analysis: After culture, cell-containing hydrogels were digested using 2 mg mL⁻¹ collagenase A (Roche) for 10 min at 37 °C. The MSC-ECFC-containing pellet was then homogenized in TRIzol reagent (Thermo Fisher Scientific) and messenger RNA (mRNA) was isolated from the aqueous phase. Potential DNA contamination was removed by a DNase treatment (Turbo DNase; Thermo Fisher) according to the manufacturer's instructions. The organoids were lysed with 350 μL RLT (Qiagen, Hilden, Germany) complemented with 1% v/v 2-Mercaptoethanol (Sigma-Aldrich), and mRNA was isolated using the RNeasy micro-kit (Qiagen), following the manufacturer's guide. The total extracted amount of mRNA was quantified with a NanoDrop ND-1000 spectrophotometer (Thermo Fisher Scientific) at 260/280 nm. Complementary DNA (cDNA) was synthesized from 1 μg mRNA using the iScript cDNA Synthesis Kit

(Bio-Rad, Hercules, USA) according to the manufacturer's instructions. qPCR analysis was executed with a Bio-Rad CFX96 Real-Time PCR Detection System (Bio-Rad) using FastStart SYBR Green Master mix (Sigma-Aldrich) and an input of 20 ng cDNA per reaction. Primers used for qPCR analysis are listed in Table S1 (Supporting Information). The amplification efficiency of the used primers was all between 0.9 and 1.1 and the relative expression was determined by the 2^{-ΔCT} formula.

For liver organoid cultures, the same protocol was followed using a Bio-Rad CFX384 Real-Time Detection System and an input of 10 ng cDNA per reaction. A housekeeping index was calculated based on a previously published formula based on GAPDH and YWHAZ.^[53]

Whole Mount Fluorescent Stainings: Prior to immunofluorescent stainings, the hydrogel constructs were permeabilized with 0.2% triton-X in PBS for 30 min and blocked in 5% BSA/PBS for 30 min. Capillary-like structures in the hydrogels were investigated by CD31 staining (5.1 μg mL⁻¹, M0823, Dako), secondary sheep antimouse biotinylated antibody (1:200, RPN1001v1, GE Healthcare), and tertiary streptavidin Alexa Fluor 488 conjugate (5.0 μg mL⁻¹, S32354, Invitrogen). In vasculogenic cocultures, ECFCs with the GFP label were not stained for CD31. The endothelial phenotype was confirmed by a rabbit antivascular endothelial cadherin antibody (VE-cad, 1:250, D87F2, Cell Signalling Technology) which was combined with a secondary donkey-antirabbit Alexa 647 antibody (5 μg mL⁻¹, ab150075, Abcam). Stabilizing cells of the capillary-like structures were identified by a mouse monoclonal Cy3-conjugated αSMA antibody (1:300 μg mL⁻¹, Clone 1A4, C6198 Sigma Aldrich). Furthermore, 4,6-diamidino-2-phenylindole (DAPI, 100 ng mL⁻¹, Sigma) was used to stain cell nuclei. The hydrogels were imaged with a confocal microscope (SP8x Leica, DMi8, Leica).

Immunohistochemistry: Fixed osteogenically differentiated hydrogels were dehydrated in graded ethanol series. After clearance in xylene, the hydrogels were embedded in paraffin and sectioned into 5 μm slices. An osteonectin staining was performed after deparaffinization and rehydration before endogenous peroxidase was blocked in 0.3% H₂O₂. Citrate buffer (pH 6) was used for antigen retrieval at 80 °C for 20 min. The primary antibody for osteonectin (4.2 μg mL⁻¹, AON-1, deposited to the DSHB by Termine, J.D.; DSHB (Developmental Studies Hybridoma Bank, created by the NICHD of the NIH and maintained at The University of Iowa, Department of Biology, Iowa City, IA 52242) Hybridoma Product AON-1^[54]) was incubated for 1 h, followed by a horseradish peroxidase-conjugated antimouse antibody (Envision + system-HRP labeled polymer, K4000 Dako). Detection of osteonectin occurred by conversion of 3,3'-diaminobenzidine solution (SK-4100, Vector) with counterstain for nuclei by hematoxylin (Merck). Concentration-matched isotype controls were performed using a mouse IgG1 monoclonal antibody (ThermoFisher Scientific).

A von Kossa staining was performed to detect mineralization of the osteogenically differentiated cocultures. After deparaffinization and rehydration, the samples were incubated with 1% silver nitrate solution (Fisher Scientific) under a light bulb for 1 h. Unreacted silver was removed by rinsing with 5% sodium thiosulfate (Alfa Aesar GmbH) for 5 min. Nuclear counterstaining was performed with hematoxylin.

The organoid-containing hydrogels were digested using 2 mg mL⁻¹ collagenase A (Roche) for 10 min at 37 °C. The organoids were fixed in 10% neutral buffered formalin, embedded in paraffin, and sections of 4 μm were cut. H&E staining (Merck KGaA, Darmstadt, Germany) was routinely performed. Imaging was performed using an Olympus microscope (CKX41) in combination with a Leica DFC425C camera.

Image Analysis: Hydrogels of vasculogenically differentiated cultures (GFP-ECFCs) were imaged at the thickest part of the hydrogel (center) on a confocal microscope (SP8x Leica, DMi8). Projections of 150 μm z-stacks were made (one stack per hydrogel, $n = 9$ stacks per condition), which were adapted in contrast and intensity with ImageJ 1.51a before batch-processing of the images. Angioquant software^[55] was used to analyse the vascular networks' total vessel length as well as average thickness of vessels by dividing the total vessel area by the total vessel length. For osteogenic cocultures, 100 μm z-stacks were made, processed in ImageJ and the total vessel length was quantified with Angioquant ($n = 9$ projections per condition).

Statistics: For mass loss studies, a one-way ANOVA was performed with a Tukey HSD post hoc analysis using Graphpad prism 7.02. For the compressive moduli, significance was determined by a Student's *t*-test in Graphpad prism 7.02. For osteogenic and hepatic cell cultures, MS Excel 2010 (Microsoft, Redmond, USA) was used for calculations and PASW Statistics 22.0 (SPSS Inc. Chicago, USA) for statistical analysis. To take into account donor variations, a mixed linear model (after log-transformation for osteogenically differentiated constructs) was conducted followed by a Bonferroni's post hoc test to compare gene expressions between the tested hydrogel types. In the model, the hydrogel type was considered as a fixed factor, while the cell donors were considered as random factors ($n = 3$ gels per group). Differences were considered statistically significant for $p < 0.05$ and the Bonferroni corrected p -values are depicted in the figures. Asterisks represent statistical significances according to p values (* $p < 0.05$; ** $p < 0.01$; *** $p < 0.001$), N refers to the number of independent experiments (with different cell donors), and n refers to the technical replicates.

Supporting Information

Supporting Information is available from the Wiley Online Library or from the author.

Acknowledgements

The authors are grateful to Mies van Steenberghe who gave support with rheological and compressive measurements at Pharmaceutical Sciences, Utrecht University. Further, Chris van Dijk (RCMU) is acknowledged for help with transduction of ECFCs with GFP. The authors acknowledge Mattie van Rijen (RCMU) for his contributions to histological stainings. This research project was partially funded by the European Union FP7-MC-IRSES "SkelGEN" project under grant agreement n°318553, and the European Research Council (ERC) (3D-JOINT, #647426). K.L. wishes to acknowledge funding by New Zealand Health Research Council Emerging Researcher First Grant (15/483).

Conflict of Interest

Co-author H.C. has the following competing financial interest to disclose; Scientific co-founder and SAB member of Surrozen (SF); SAB member of Merus, Utrecht; SAB member of Kallyope, NY; SAB member of Decibel, Boston; And the following non-financial interests; Venture partner of LSP, Amsterdam; Inventor on multiple patents related to Lgr5 stem cells and organoids.

Keywords

FXIII, gelatin, liver organoids, Matrigel, osteogenesis, polyethylene glycol, vasculogenesis

Received: July 23, 2019

Published online: August 12, 2019

- [1] I. V. Yannas, E. Lee, D. P. Orgill, E. M. Skrabut, G. F. Murphy, *Proc. Natl. Acad. Sci. U S A* **1989**, *86*, 933.
 [2] a) D. Saris, A. Price, W. Widuchowski, M. Bertrand-Marchand, J. Caron, J. O. Drogset, P. Emans, A. Podskubka, A. Tsuchida, S. Kili, D. Levine, M. Brittberg, S. s. group, *Am. J. Sports Med.* **2014**, *42*, 1384; b) E. Basad, B. Ishaque, G. Bachmann, H. Sturz,

- J. Steinmeyer, *Knee Surg. Sports Traumatol. Arthroscopy* **2010**, *18*, 519.
 [3] A. Atala, S. B. Bauer, S. Soker, J. J. Yoo, A. B. Retik, *Lancet* **2006**, *367*, 1241.
 [4] a) A. Shafiee, A. Atala, *Annu. Rev. Med.* **2017**, *68*, 29; b) A. Jaklencic, A. Stamp, E. Deweerdt, A. Sherwin, R. Langer, *Tissue Eng., Part B* **2012**, *18*, 155; c) J. Rouwkema, A. Khademhosseini, *Trends Biotechnol.* **2016**, *34*, 733.
 [5] A. Fatehullah, S. H. Tan, N. Barker, *Nat. Cell Biol.* **2016**, *18*, 246.
 [6] a) L. G. Villa-Diaz, A. M. Ross, J. Lahann, P. H. Krebsbach, *Stem Cells* **2013**, *31*, 1; b) H. K. Kleinman, G. R. Martin, *Semin. Cancer Biol.* **2005**, *15*, 378.
 [7] C. S. Hughes, L. M. Postovit, G. A. Lajoie, *Proteomics* **2010**, *10*, 1886.
 [8] X. L. Yin, B. E. Mead, H. Safaee, R. Langer, J. M. Karp, O. Levy, *Cell Stem Cell* **2016**, *18*, 25.
 [9] Y. Kubota, H. K. Kleinman, G. R. Martin, T. J. Lawley, *J. Cell Biol.* **1988**, *107*, 1589.
 [10] E. Polykandriotis, A. Arkudas, R. E. Horch, U. Kneser, *Am. J. Pathol.* **2008**, *172*, 1441.
 [11] G. Benton, I. Arnaoutova, J. George, H. K. Kleinman, J. Koblinski, *Adv. Drug Delivery Rev.* **2014**, *79-80*, 3.
 [12] K. Schneeberger, B. Spee, P. Costa, N. Sachs, H. Clevers, J. Malda, *Biofabrication* **2017**, *9*, 013001.
 [13] a) N. Gjorevski, N. Sachs, A. Manfrin, S. Giger, M. E. Bragina, P. Ordonez-Moran, H. Clevers, M. P. Lutolf, *Nature* **2016**, *539*, 560; b) E. H. Nguyen, W. T. Daly, N. N. T. Le, M. Farnoodian, D. G. Belair, M. P. Schwartz, C. S. Lebakken, G. E. Ananiev, M. A. Saghiri, T. B. Knudsen, N. Sheibani, W. L. Murphy, *Nat. Biomed. Eng.* **2017**, *1*, pii: 0096; c) R. Cruz-Acuna, M. Quiros, A. E. Farkas, P. H. Dedhia, S. Huang, D. Siuda, V. Garcia-Hernandez, A. J. Miller, J. R. Spence, A. Nusrat, A. J. Garcia, *Nat. Cell Biol.* **2017**, *19*, 1326.
 [14] A. M. Rosales, K. S. Anseth, *Nat. Rev. Mater.* **2016**, *1*, pii: 15012.
 [15] a) R. P. Mecham, *Curr. Protoc. Cell Biol.* **2012**, Chapter 10, Unit 10.1; b) P. Lu, K. Takai, V. M. Weaver, Z. Werb, *Cold Spring Harbor Perspect. Biol.* **2011**, *3*, a005058; c) T. Rozario, D. W. DeSimone, *Dev. Biol.* **2010**, *341*, 126.
 [16] Y. Kim, H. Ko, I. K. Kwon, K. Shin, *Int. Neurolog. J.* **2016**, *20*, S23.
 [17] a) A. O. Elzoghby, *J. Controlled Release* **2013**, *172*, 1075; b) M. C. Oz, D. M. Cosgrove, B. R. Badduke, J. D. Hill, M. R. Flannery, R. Palumbo, N. Topic, F. M. S. Grp, *Ann. Thoracic Surg.* **2000**, *69*, 1376.
 [18] M. Ehrbar, A. Sala, P. Lienemann, A. Ranga, K. Mosiewicz, A. Bittermann, S. C. Rizzi, F. E. Weber, M. P. Lutolf, *Biophys. J.* **2011**, *100*, 284.
 [19] a) Y. C. Chen, R. Z. Lin, H. Qi, Y. Z. Yang, H. J. Bae, J. M. Melero-Martin, A. Khademhosseini, *Adv. Funct. Mater.* **2012**, *22*, 2027; b) P. Occhetta, R. Visone, L. Russo, L. Cipolla, M. Moretti, M. Rasponi, *J. Biomed. Mater. Res., Part A* **2015**, *103*, 2109; c) U. Blache, Q. Vallmajo-Martin, E. R. Horton, J. Guerrero, V. Djonov, A. Scherberich, J. T. Erler, I. Martin, J. G. Snedeker, V. Milleret, M. Ehrbar, *EMBO Rep.* **2018**, *19*, e45964.
 [20] J. Rouwkema, J. de Boer, C. A. Van Blitterswijk, *Tissue Eng.* **2006**, *12*, 2685.
 [21] a) M. Kolbe, Z. Xiang, E. Dohle, M. Tonak, C. J. Kirkpatrick, S. Fuchs, *Tissue Eng., Part A* **2011**, *17*, 2199; b) B. J. Klotz, K. S. Lim, Y. X. Chang, B. G. Soliman, I. Pennings, F. P. W. Melchels, T. B. F. Woodfield, A. J. Rosenberg, J. Malda, D. Gawlitta, *Eur. Cells Mater.* **2018**, *35*, 335; c) D. Gawlitta, J. O. Fledderus, M. H. van Rijen, I. Dokter, J. Alblas, M. C. Verhaar, W. J. Dhert, *Tissue Eng., Part A* **2012**, *18*, 208; d) U. Blache, S. Metzger, Q. Vallmajo-Martin, I. Martin, V. Djonov, M. Ehrbar, *Adv. Healthcare Mater.* **2016**, *5*, 489.
 [22] a) K. Cameron, R. Tan, W. Schmidt-Heck, G. Campos, M. J. Lyall, Y. Wang, B. Lucendo-Villarín, D. Szkolnicka, N. Bates, S. J. Kimber,

- J. G. Hengstler, P. Godoy, S. J. Forbes, D. C. Hay, *Stem Cell Rep.* **2015**, 5, 1250; b) L. K. Kanninen, R. Harjumaki, P. Peltoniemi, M. S. Bogacheva, T. Salmi, P. Porola, J. Niklander, T. Smutny, A. Urtili, M. L. Yliperttula, Y. R. Lou, *Biomaterials* **2016**, 103, 86.
- [23] C. A. Rubio, *In Vivo* **1998**, 12, 183.
- [24] a) S. E. Sakiyama, J. C. Schense, J. A. Hubbell, *FASEB J.* **1999**, 13, 2214; b) J. C. Schense, J. A. Hubbell, *Bioconjugate Chem.* **1999**, 10, 75.
- [25] a) M. Ehrbar, S. C. Rizzi, R. Hlushchuk, V. Djonov, A. H. Zisch, J. A. Hubbell, F. E. Weber, M. P. Lutolf, *Biomaterials* **2007**, 28, 3856; b) M. Ehrbar, S. C. Rizzi, R. G. Schoenmakers, B. S. Miguel, J. A. Hubbell, F. E. Weber, M. P. Lutolf, *Biomacromolecules* **2007**, 8, 3000.
- [26] W. S. Hur, N. Mazinani, X. J. Lu, H. M. Britton, J. R. Byrnes, A. S. Wolberg, C. J. Kastrup, *Blood* **2015**, 126, 2329.
- [27] a) D. F. Torchiana, *J. Cardiac Surg.* **2003**, 18, 504; b) J. M. Harris, *Poly (Ethylene Glycol) Chemistry: Biotechnical and Biomedical Applications*, Plenum Press, New York **1992**.
- [28] a) M. A. Daniele, A. A. Adams, J. Naciri, S. H. North, F. S. Ligler, *Biomaterials* **2014**, 35, 1845; b) Y. Fu, K. D. Xu, X. X. Zheng, A. J. Giacomini, A. W. Mix, W. Y. J. Kao, *Biomaterials* **2012**, 33, 48.
- [29] a) F. Anjum, P. S. Lienemann, S. Metzger, J. Biernaskie, M. S. Kallos, M. Ehrbar, *Biomaterials* **2016**, 87, 104; b) A. Ranga, M. P. Lutolf, J. Hilborn, D. A. Ossipov, *Biomacromolecules* **2016**, 17, 1553; c) H. P. Tan, M. Fan, Y. Ma, J. C. Qiu, X. M. Li, J. X. Yan, *Adv. Healthcare Mater.* **2014**, 3, 1769.
- [30] a) C. C. Lin, K. S. Anseth, *Adv. Funct. Mater.* **2009**, 19, 2325; b) P. S. Lienemann, M. P. Lutolf, M. Ehrbar, *Adv. Drug Delivery Rev.* **2012**, 64, 1078.
- [31] a) K. M. Park, Y. Lee, J. Y. Son, D. H. Oh, J. S. Lee, K. D. Park, *Biomacromolecules* **2012**, 13, 604; b) C. B. Hutson, J. W. Nichol, H. Aubin, H. Bae, S. Yamanlar, S. Al-Haque, S. T. Koshy, A. Khademhosseini, *Tissue Eng., Part A* **2011**, 17, 1713.
- [32] S. S. Soofi, J. A. Last, S. J. Liliensiek, P. F. Nealey, C. J. Murphy, *J. Struct. Biol.* **2009**, 167, 216.
- [33] S. Levenberg, J. Rouwkema, M. Macdonald, E. S. Garfein, D. S. Kohane, D. C. Darland, R. Marini, C. A. van Blitterswijk, R. C. Mulligan, P. A. D'Amore, R. Langer, *Nat. Biotechnol.* **2005**, 23, 879.
- [34] Y. Mousseau, S. Mollard, H. Qiu, L. Richard, R. Cazal, A. Nizou, N. Vedrenne, S. Remi, Y. Baaj, L. Fourcade, B. Funalot, F. G. Sturtz, *Lab. Invest.* **2014**, 94, 340.
- [35] M. Simons, *Circulation* **2005**, 111, 1556.
- [36] R. Kalluri, *Nat. Rev. Cancer* **2003**, 3, 422.
- [37] B. J. Kang, H. H. Ryu, S. S. Park, Y. Kim, H. M. Woo, W. H. Kim, O. K. Kweon, *J. Vet. Med. Sci.* **2012**, 74, 827.
- [38] a) I. Gotman, D. Ben-David, R. E. Unger, T. Bose, E. Y. Gutmanas, C. J. Kirkpatrick, *Acta Biomater.* **2013**, 9, 8440; b) N. Celikkin, S. Mastrogiacomo, J. Jaroszewicz, X. F. Walboomers, W. Swieszkowski, *J. Biomed. Mater. Res., Part A* **2018**, 106, 201.
- [39] a) L. Zhou, G. Tan, Y. Tan, H. Wang, J. Liao, C. Ning, *RCS Adv.* **2014**, 4, 21997; b) P. Zhu, Y. Masuda, K. Koumoto, *Biomaterials* **2004**, 25, 3915.
- [40] a) K. Bougas, V. F. Stenport, F. Currie, A. Wennerberg, *J. Oral Maxillofac. Res.* **2011**, 2, e3; b) K. Bougas, V. F. Stenport, F. Currie, A. Wennerberg, *J. Oral Maxillofac. Res.* **2012**, 2, e5.
- [41] M. G. Lampugnani, M. Resnati, M. Raiteri, R. Pigott, A. Pisacane, G. Houen, L. P. Ruco, E. Dejana, *J. Cell Biol.* **1992**, 118, 1511.
- [42] E. S. Harris, W. J. Nelson, *Curr. Opin. Cell Biol.* **2010**, 22, 651.
- [43] M. Kolbe, Z. Xiang, E. Dohle, M. Tonak, C. J. Kirkpatrick, S. Fuchs, *Tissue Eng., Part A* **2011**, 17, 2199.
- [44] a) M. Huch, H. Gehart, R. van Bortel, K. Hamer, F. Blokzijl, M. M. Versteegen, E. Ellis, M. van Wenum, S. A. Fuchs, J. de Ligt, M. van de Wetering, N. Sasaki, S. J. Boers, H. Kemperman, J. de Jonge, J. N. Ijzermans, E. E. Nieuwenhuis, R. Hoekstra, S. Strom, R. R. Vries, L. J. van der Laan, E. Cuppen, H. Clevers, *Cell* **2015**, 160, 299; b) M. Huch, C. Dorrell, S. F. Boj, J. H. van Es, V. S. Li, M. van de Wetering, T. Sato, K. Hamer, N. Sasaki, M. J. Finegold, A. Haft, R. G. Vries, M. Grompe, H. Clevers, *Nature* **2013**, 494, 247.
- [45] M. Huch, H. Gehart, R. van Bortel, K. Hamer, F. Blokzijl, M. M. A. Versteegen, E. Ellis, M. van Wenum, S. A. Fuchs, J. de Ligt, M. van de Wetering, N. Sasaki, S. J. Boers, H. Kemperman, J. de Jonge, J. N. M. Ijzermans, E. E. S. Nieuwenhuis, R. Hoekstra, S. Strom, R. R. G. Vries, L. J. W. van der Laan, E. Cuppen, H. Clevers, *Cell* **2015**, 160, 299.
- [46] O. Chaudhuri, L. Gu, D. Klumpers, M. Darnell, S. A. Bencherif, J. C. Weaver, N. Huebsch, H. P. Lee, E. Lippens, G. N. Duda, D. J. Mooney, *Nat. Mater.* **2016**, 15, 326.
- [47] J. Groll, T. Boland, T. Blunk, J. A. Burdick, D. W. Cho, P. D. Dalton, B. Derby, G. Forgacs, Q. Li, V. A. Mironov, L. Moroni, M. Nakamura, W. Shu, S. Takeuchi, G. Vozzi, T. B. Woodfield, T. Xu, J. J. Yoo, J. Malda, *Biofabrication* **2016**, 8, 013001.
- [48] a) W. Schuurman, V. Khristov, M. W. Pot, P. R. van Weeren, W. J. A. Dhert, J. Malda, *Biofabrication* **2011**, 3, 021001; b) J. Visser, F. P. W. Melchels, J. E. Jeon, E. M. van Bussel, L. S. Kimpton, H. M. Byrne, W. J. A. Dhert, P. D. Dalton, D. W. Huttmacher, J. Malda, *Nat. Commun.* **2015**, 6, 6933; c) N. V. Mekhileri, K. S. Lim, G. C. J. Brown, I. Mutreja, B. S. Schon, G. J. Hooper, T. B. F. Woodfield, *Biofabrication* **2018**, 10, 024103.
- [49] N. Gjorevski, M. P. Lutolf, *Nat. Protoc.* **2017**, 12, 2263.
- [50] a) M. P. Lutolf, N. Tirelli, S. Cerritelli, L. Cavalli, J. A. Hubbell, *Bioconjugate Chem.* **2001**, 12, 1051; b) M. Ehrbar, A. Sala, P. Lienemann, A. Ranga, K. Mosiewicz, A. Bittermann, S. C. Rizzi, F. E. Weber, M. P. Lutolf, *Biophys. J.* **2011**, 100, 284.
- [51] K. S. Lim, M. H. Alves, L. A. Poole-Warren, P. J. Martens, *Biomaterials* **2013**, 34, 7097.
- [52] a) A. Nilasaroya, L. A. Poole-Warren, J. M. Whitelock, P. Jo Martens, *Biomaterials* **2008**, 29, 4658; b) K. S. Lim, J. Kundu, A. Reeves, L. A. Poole-Warren, S. C. Kundu, P. J. Martens, *Macromol. Biosci.* **2012**, 12, 322.
- [53] M. W. Pfaffl, A. Tichopad, C. Prgomet, T. P. Neuvians, *Biotechnol. Lett.* **2004**, 26, 509.
- [54] M. E. Bolander, P. G. Robey, L. W. Fisher, K. M. Conn, B. S. Prabhakar, J. D. Termine, *Calcif. Tissue Int.* **1989**, 45, 74.
- [55] A. Niemisto, V. Dunmire, O. Yli-Harja, W. Zhang, I. Shmulevich, *IEEE Trans. Med. Imaging* **2005**, 24, 549.